Discover Water

Research

Potential toxic effects linked to taurine interactions with alkanolamines and diisopropylamine

Erica Pensini[1,2] · **Caitlyn Hsiung**[1] · **Nour Kashlan**[1]

Received: 25 July 2024 / Accepted: 8 October 2024
Published online: 18 October 2024
© The Author(s) 2024 OPEN

Abstract

Diisopropylamine (DIPA), aminomethyl propanol (AMP), amino ethoxy ethanol (AEE), diethanolamine (DEA), ethanolamine (EA), pyridine (PYR) and methyl diethanolamine (MDEA) are used for carbon capture and to sweeten sour gas, and are found in groundwater. They are also used in cosmetic products. Taurine is abundant in the body, with key biological functions linked to its charged SO groups. Interactions between SO and amines have not been studied, but can strongly affect the biological function of taurine. Fourier transform infrared spectroscopy indicates SO…HN hydrogen bonding between taurine and DIPA, AMP, AEE, DEA, EA and MDEA. These interactions induce the formation of hydrophobic amine-taurine clusters, thus decreasing amine miscibility in water, as revealed by light scattering. This effect is most marked for DIPA, leading to turbid mixtures indicative of micron-sized droplets. PYR and taurine likely interact via S…N bonding. This study offers insights regarding potential mechanisms of amine toxicity to humans.

Graphical Abstract

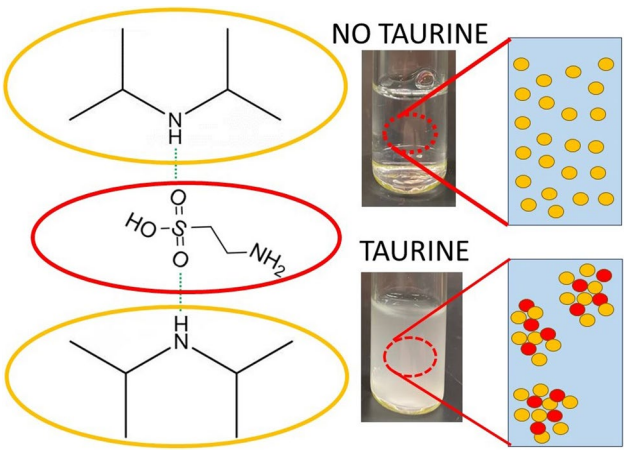

Supplementary Information The online version contains supplementary material available at https://doi.org/10.1007/s43832-024-00146-1.

✉ Erica Pensini, epensini@uoguelph.ca | [1]School of Engineering, College of Engineering and Physical Sciences, University of Guelph, 50 Stone Rd E, Guelph, ON N1G 2W1, Canada. [2]Biophysics Interdepartmental Group (BIG), University of Guelph, 50 Stone Road East, Guelph, ON) N1G 2W1, Canada.

Keywords Taurine · Groundwater pollution · Amines · Attenuated total reflectance—Fourier transform infrared spectroscopy · Molecular interactions

1 Introduction

Taurine is a β-amino acid biosynthesized from cysteine [1]. The structure of taurine is shown in Scheme 1. Taurine comprises both an -NH_2 and a sulfate group, dissimilar to most other amino acids. This difference affects the physical properties of taurine, and hence its diffusion, solubility, ionization, and isoelectric points [2]. It also renders taurine strongly zwitterionic, with high water solubility and low lipophility. Also, sulfonation is important because it imparts a permanent negative charge to taurine at physiologically relevant pH values, thus inhibiting passive diffusion of taurine across biological membranes [2]. Mammals use a transporter (TauT) to move taurine across membranes.

Taurine is a non essential amino acid, because it is not used to build proteins in the body. Nonetheless, it is a functional amino acid, serving important biological functions. It is present in significant amounts freely floating in the intracellular water of the cells. For instance, the concentration of taurine in cardiac tissue is ≥ 20 mM [3]. Lack of taurine has been associated with cardiac dysfunction, as well as with atrophy of other muscles [4]. For example, taurine regulates proper function of skeletal muscles [5], and knockout of the taurine transporter gene in mice decreases exercise capacity and impairs skeletal muscle [2]. Lack of taurine has also been associated with premature aging and reproductive impairments [1]. Moreover, taurine plays an important role in lung function [4]. A study proposes that taurine is an osmoregulator of cell volume, for instance in fish, as well as in the brain under high osmotic states (e.g., hypernatremia, dehydration and uremia) [3]. Another study also reports that taurine aids in cell volume restoration following osmotic perturbation [4]. Furthermore, taurine controls proper function of adrenal glands [2]. Taurine action on the adrenal gland is linked to its sulfonate group, rather than on its amino group [2]. It has been proposed that the biological activity of analogs and homologs of taurine requires the simultaneous presence of an unsubstituted amine and a sulfonate group, or of an unsubstituted amine and a sulfinate group [2]. Taurine is particularly abundant in the retina and plays a key role in maintaining both the function of the retina [6] and the tapetum (i.e., the membrane located behind the retina, which reflects back the light that has gone through the retinal cell layers and thus enhances light detection by photoreceptor cells) [1]. Visual dysfunction in humans and animals is linked to taurine deficiency and can be reversed with nutritional supplements [6]. Although taurine can be produced in the body starting from cysteine [2], human children are dependent on dietary taurine more than adults [6]. This may explain taurine abundance in human breast milk [3]. Taurine abundance in human milk is also justified by the fact that it is particularly essential to development of the fetus and newborn, and specifically for human fetal brain neuron proliferation and differentiation [2]. Another study reports that in mitochondria, the pH gradient across the inner-membrane is stabilised by buffering of the matrix [7]. The authors found that the pKa value of taurine is 9.0 at 25 °C and 8.6 at 37 °C, and that taurine can act as a buffer in the mitochondrial matrix, thus rendering it a biochemical reaction chamber suitable for enzymes [7]. For example, the authors found that acyl-CoA dehydrogenase enzymes have optimal activity in a taurine buffer. These enzymes have a key role in the beta-oxidation of fatty acids [7]. The authors propose that taurine depletion is linked to mitochondrial dysfunction and diabetes [7]. Taurine has also been found to decrease cholesterol levels and fat [2]. Taurine plays a key role in the nervous system and on cognitive functions [8]. Taurine supplements have been found to markedly improve and even restore cognition loss [9]. Nonetheless, excessively high elevated taurine level in cerebrospinal fluid by exogenous administration causes cognition retardation between the perinatal to early postnatal period, although not outside this life period [9]. Another study also reports that when neutrophils are activated during inflammation, taurine reacts with hypochloric acid and forms taurine chloramine, thus triggering anti-inflammatory responses in the body [5]. Finally, taurine was found to enhance

Scheme 1 Structure of taurine, a non-essential amino acid with important biological functions

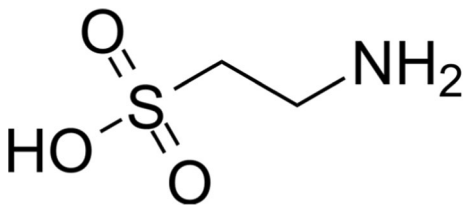

the function of leucocytes after chemotherapy of cyclophosphamide of individuals affected by malignant tumors [10]. While this summary is not exhaustive, it offers a glimpse into the numerous functions of taurine in the body.

Given the different important functions of taurine, and its peculiar structure (which comprises a sulfate group), we are interested in probing its interactions with alkanolamines and diisoproylamine, an aliphatic amine. Such interactions could affect the functionality of taurine in the body, thus harming human and animal health. Alkanolamines and DIPA are used to sweeten sour gas and crude oil (i.e., to remove acidic components that would hamper their use), and for carbon capture [11–14]. They are found in groundwater close to industrial sites [15–17], and in plants growing in impacted areas [18]. For example, a study reports that DIPA (as well as sulfolane) were found in a wetland close to a sour-gas processing facility, as well as in plants growing in this area [18]. DIPA concentrations were 16 mg/kg in sedge flower heads, and 15–17 mg/kg and 0.2–1.0 mg/L in soil and groundwater, respectively [18]. Plants could be eaten by wildlife, with potential risks. Beyond their presence in groundwater due to accidental spills or improper management, alkanolamines are used as in different cosmetic products, such as hair dyes, shampoos, and lotions [17, 19], as well as in laundry products [20]. For example, alkanolamines are used in hair dyes as pH adjusters [21]. A patent describing hair color composition indicates that suggested ranges of pH adjusters such as EA and AMP are from about 0.00001–8% by weight of the total composition [22]. Moreover, EA is used as a pearlizing agent (to create a pearlescent effect in products, for visual appeal) in oxidizing hair dyes, and a patent recommends amounts ranging from about 0.01% to about 10% by weight of the formulation [23]. EA is also used to combat skin aging, and suggested concentrations range from 0.01% to about 10% [24]. Concentrations up to 10wt% are also proposed for AMP in skin formulations [25]. This will lead to dermal exposure. Also, when septic tanks rather than water treatment facilities are used, chemicals present in household products will be released in groundwater. Similarly, DIPA is commercialized for various applications, including as an intravenous antihypertensive agent [26] and in contact lens cleaner applications [27]. Also, its has been used for adjusting pH in cosmetic formulations, in colognes, and toilet cleaners [28]. Dow Chemicals commercializes DIPA for products serving as emulsifiers, stabilizers, chemical intermediates and neutralizers, both for industrial applications and in household cleaning product. The toxicity of the many constituents in household cleaning products, cosmetics and colognes should be more strictly regulated. While this study focuses on amines, other constituents in common products also have adverse environmental impacts, such as fragrances [29]. A study conducted on rats and rabbits reports that the peroral LD50 of alkanolamines is 1.07–5.66 mL/kg, while the percutaneous LD50 0.57–10.2 mL/kg [30]. LD50 (lethal dose 50) represents the amount of a substance that kills 50% of a test sample upon exposure, in this case through ingestion (peroral) or through the skin (percutaneous). In other words, this experiment corresponds to the ingestion of ≈60–300 mL of alkanolamines by a group of individuals weighing 60 kg, to observe the death of 50% of the individuals studied. Gagnaire et al. conduced a study on mice, without anaesthesia, to identify the amounts of aliphatic amines resulting in a 50% decrease in the respiratory rate (RD50) [31]. The RD50 values associated with exposure to saturated amines ranged from 50 to 200 ppm.

In the case of DIPA, the National Institute for Occupational Safety and Health (NIOSH) sets the REL (recommended exposure limit) TWA (time weighted average) through dermal exposure to 5 ppm. NIOSH reports that exposure routes for DIPA are inhalation, skin absorption, ingestion, skin and/or eye contact, and symptoms include irritation of the eyes, skin, respiratory system, nausea, vomiting, headache and visual disturbance. Target organs include the eyes, the skin, and the respiratory system.

A non-cancer inhalation chronic toxicity assessment was conducted on rats and mice using diethanolamine (DEA), and found that DEA mainly acts as a respiratory irritant with effects occurring in the upper respiratory tract [32]. Values were extrapolated from mice and rats to humans, and the chronic Reference Value for DEA was estimated to be 11 ppb (33 µg/m^3). Another study reports that DEA adversely affects the crustacean Calanus finmarchicus, altering the transcription of genes involved in lipid metabolism, antioxidant systems, metal binding, and amino acid and protein catabolism [33]. Interestingly, the authors also report altered expression of fatty acid derivates, of the amino acids threonine, methionine, glutamine, arginine, alanine and leucine, as well as of cholines (choline, phosphocholine and glycerophosphocholine) [33]. The authors did not discuss the effects of DEA on taurine [33]. A study was conducted on rat dams (pregnant females), exposing the mothers to MDEA during pregnancy [34]. The study showed dose-dependent skin irritation at 250 mg/kg/day, as well as decreased erythrocyte, hemoglobin, and hematocrit count upon exposure to 1000 mg/kg/day. A study found that, after exposure, MDEA is sequestered in the skin, resulting in delayed and steady release into the bloodstream, from which it migrates to the liver and kidneys [35]. Ballantyne et al. report that the dermal LD50s for MDEA were 10.2 g/kg bw (9.85 ml/kg bw) and 11.34 g/kg bw (10.90 ml/kg bw) in a 24 h study in male and female rabbits, respectively [36]. Exposure led to adverse dermal effects, lung, liver and kidney damage. When dams (pregnant female mice) were exposed to 750 and 1000 mg/kg bw/day, they became anemic. Leung and Ballantyne, 1998 report that the NOAELs for maternal toxicity and embryofetal toxicity is 250 mg/kg bw/day and teratogenicity occurs at 1000 mg/kg

bw/day, respectively [37]. The LD50 of EA in rats is 1.1–2.7 g/kg body weight [38]. Repeated exposure caused adverse behavioural effects and degenerative changes in different organs, mostly in the liver and kidneys [39], as well as skin and respiratory irritation. EA is mainly metabolized through the liver, followed by the heart and brain [40]. Exposure to EA also adversely affects spermatogenesis, and causes malformations and intrauterine deaths [41]. Another study analyzed the oxidative and CO_2-mediated degradation for 75 days, during CO_2 capture by amines. This study reports that exposure to oxidatively degraded EA caused inflammatory cytokine expression [42]. AMP affects the formation of free fatty acids from lipids. When rats fed a choline deficient diet were dosed with AMP, they suffered from inhibited fat catabolism and increased amount of hepatic lipid, as well as an increased fat content of the liver [43]. The LD50 of AMP reported is 2.9 g/kg for rats and 2.15 g/kg for mice [43]. A study reports that AMP in the blood decreased by roughly 80% AMP in a 4-h period, followed by slower elimination of AMP incorporated into phospholipids and other cellular fractions. AMP secreted from the body was unchanged [44].

In summary, DIPA and alkanolamines can be released in the environment due to accidental spills. They are also found in varying cosmetic products, which come in direct contact with the skin and could be accidentally ingested. Also, such products will be released in groundwater in all cases where household wastewater is treated with basic treatment units, such as septic tanks, rather than in suitable wastewater treatment facilities. Many animal studies have attempted to assess the toxicity of alkanolamines and diisopropylamine on the body. In these studies, animals were exposed to high or even lethal doses. This approach can provide an indication of toxicity. Nonetheless, it does not give information about the mechanisms involved in the toxic effects observed, beyond uncertainties in correlating responses of humans to that of other animal species, and animal welfare considerations. The notable editorial 'Spare the animals and explore the alternatives' published in Nature in 2024 speaks to this point [45]. Understanding the ramifications of exposure to chemicals on health would benefit from assessing their interactions with relevant biological molecules, of which taurine is an example. The complexity of organisms doubtlessly renders this analysis only one of the many steps required to understand the mechanisms of toxicity. Nonetheless, our current study aims to probe the effect of alkanolamines and DIPA in a way different from typical animal studies, thereby offering a complementary perspective. Specifically, in this study we highlight how alkanolamines and DIPA interact with the sulfate group of taurine. As mentioned earlier, this group is key for the biological function of taurine.

2 Materials and methods

2.1 Materials

AMP (for synthesis), diethanolamine (DEA, ≥ 99%), MDEA (≥ 99%), AEE (for synthesis), pyridine (PYR, ≥ 99% purity) ethanolamine (EA, ≥ 99%), diisopropylamine (DIPA, for synthesis), and Nile red were purchased from Sigma Aldrich (Canada). Cavity slides (EISCO) were also purchased from Sigma Aldrich (Canada). Taurine (99% purity) and toluene (certified ACS) were purchased for Fisher Scientific (Canada). Milli-Q was used in all experiments conducted, except part of attenuated total reflectance-Fourier transform infrared spectroscopy experiments, as described in Sect. 2.2.

2.2 Attenuated total reflectance-Fourier transform infrared spectroscopy (ATR-FTIR)

ATR-FTIR measurements were conducted to analyze mixtures containing taurine and water, as well as taurine, amines and water. The following samples were analyzed: 1) binary mixtures with water (with 50wt% amine in water), using AMP, DEA, MDEA, AEE, PYR, EA and DIPA; 2) ternary mixtures with taurine, amines and water (at a 1:1:1 wt. ratio of taurine:amine:water), using AMP, DEA, MDEA, AEE, PYR, EA and DIPA; 3) binary mixtures of DIPA and D_2O (with 50wt% amine in D_2O) and ternary mixtures with taurine, DIPA and water (at a 1:1:1 wt. ratio of taurine:amine: D_2O). Experiments were conducted using D_2O to avoid overlap between the δ(HOH) band of water and bands contributed by the NH groups of DIPA. Absorbance spectra were collected using an ATR-FTIR spectrometer (Thermoscientific Nicolet Summit FTIR spectrometer with an Everest ATR), with an accompanying IR solution software. Each spectrum is the average of 32 scans for all amines except DIPA, with a resolution of 2 cm^{-1}, in the wavenumber range of 400 cm^{-1} to 4000 cm^{-1}. Due to the high volatility of DIPA, 10 scans were taken. In all cases, ATR-FTIR spectra were processed using Quasar Orange, which is a freely available software [46, 47], normalizing relevant absorbance bands, after applying a rubber band baseline correction. Furthermore, the DO stretch band of D_2O was deconvolved using five Gaussian peaks, by minimizing the difference between the simulated and the experimental spectra using Excel Solver and the

GRG non-linear solving method. A sample fit is provided in the supporting information file (Fig. S1). The Gaussian peaks associated with each of the five ranges of wavenumbers analyzed represent D_2O molecules coordinated differently through hydrogen (H) bonds with other molecules in solution, either taurine, DIPA or other D_2O molecules, as further described in the results and discussion section. We call 'species' D_2O molecules with a different coordination. The relative area of each peak is thus representative of the abundance of each D_2O 'species'. The area under each Gaussian peak is estimated using the amplitude (AMPL) and the standard deviation (SD), as Area = AMPL·SD/0.3989. The relative areas are obtained by dividing the area of each Gaussian by the sum of the areas under all five peaks convolved under the DO stretch band. These were lumped into three groups, at low, mid and high wavenumbers, 2570–2690 cm^{-1}, 2400–2500 cm^{-1} and 2220–2240 cm^{-1}, indicative of hydrogen bonding in D_2O. The deconvolution of the DO stretch band of D_2O was conducted for two to five independent replicates for each type of sample analyzed, and these replicates were used to estimate the averages and the error bars provided in the results and discussion section. The supporting information file reports the peak positions of the peaks convolved under the υ(DO) stretch band of D_2O, for each replicate experiments. All experiments were conducted in duplicate at least.

2.3 Turbidity measurements

Turbidity measurements were conducted to determine the effect of taurine on toluene emulsification by alkanolamines and DIPA. Measurements were conducted using a spectrophotometer (SPECTRONIC™ 200 Spectrophotometer, Fisher Scientific, Canada) at a 505 nm wavelength, using quartz cuvettes. Samples were prepared with either 1wt% taurine (relative to water) or without taurine, with 1wt% toluene (relative to the aqueous phase) and with 10wt% amines (relative to water). Samples were agitated by hand for 10 s, after which they were allowed to settle for 2 min. Measurements were taken at 2 min and 3 min, and the average of at least two independent replicates was used. Milli-Q water was used as the background.

2.4 Bottle tests

Bottle tests were conducted without taurine and with 1wt% taurine (relative to water), with 10wt% and 18wt% amines, with and without toluene (1:4 toluene:aq. solution, wt. based). Samples were agitated by hand for 60 s and allowed to settle for up to 24 h, after which they were analyzed using light scattering, as described in Sect. 2.6.

2.5 COSMO-RS (conductor-like screening model for realistic solvation)

COSMO-RS was used to estimate the solubility of toluene in the different amines used. COSMO-RS (http://www.scm.com) was developed by Vrije Universiteit, Amsterdam.

2.6 Light scattering

Light scattering was conducted using a Malvern Zetasizer Nano ZSP at 20^{O}C, using quartz cuvettes. Measurements were conducted at least in triplicate. Light scattering experiments were conducted to estimate the size of amine droplets in water, in samples containing 20wt% amines and 1wt% taurine, relative to water. The refractive indexes used were as follows: 1.392 for DIPA, 1.449 for AMP, 1.454 for AEE, 1.454 for AE, 1.477 for DEA, 1.469 for MDEA, and the refractive index of water was 1.33 [48].

2.7 Optical microscopy

An optical VHX-5000 digital microscope (Keyence) was used to image DIPA-water mixtures, prepared with 70wt% DIPA and 2wt% taurine, relative to the water phase. Images were taken using samples stained with Nile red. Nile red stains DIPA, but not water. It was added to qualitatively differentiate between the composition of droplets and the continuous phase. Images were also taken for stained samples containing 10wt% DIPA, 1wt% toluene, 2 wt% taurine, for comparison. Samples were imaged using cavity slides, immediately after mixing the samples.

3 Results and discussion

Section 3.1 analyzes interactions between taurine and amines in aqueous solutions using ATR-FTIR. Specifically, we probe interactions between amines and the SO group of taurine, which serves important biological functions. We also analyze taurine-amine interactions to explain the effect of taurine on the miscibility of amines in water, discussed in Sect. 3.2. In Sect. 3.2, we also highlight the potential implications of this effect on amine toxicity.

3.1 ATR-FTIR analysis of taurine-amine interactions

We use ATR-FTIR to understand taurine-amine interactions in water, focusing on the S=O band (Fig. 1). As discussed in the introduction, the sulfate group plays a key role in the biological function of taurine. In Fig. 1, the band at 1000–1100 cm^{-1} is attributed to υ (SO) [49]. In neat taurine, the SO band is split into a peak at 1034 cm^{-1} and a shoulder at 1042 cm^{-1}, both of which are ascribed to the stretching vibration of the sulfate groups, υ (SO) [50, 51]. We propose that the two bands correspond to bonds having different strength, with the highest wavenumbers corresponding to stronger S=O bonds. Upon mixing with water (without amines), the band at 1034 cm^{-1} disappears, while the intensity of the peak at 1042 cm^{-1} increases. Intermolecular hydrogen (H) bonding between the oxygen of S=O groups and other molecules would elongate and weaken S=O bonds, shifting the υ (SO) band to lower wavenumbers. Here, the opposite effect is observed, thus indicating weakening of H bonding between SO and other molecules upon mixing in water, consistent with previous studies [49, 52–54]. These studies report that taurine interacts with water both through the SO groups (H bond acceptors) and through the NH groups (H bond donors) [52–54], but H bonds with SO groups are weak [49]. Note that a shift of υ (SO) to higher wavenumbers would also be observed if interactions occurred through the sulfur atom [55]. However, while H bonding between the oxygen of S = O groups and the hydrogen of water was previously reported [56–59], H bonding between water and the sulfur atom of taurine is unlikely.

Taurine is immiscible in pure amines, but interacts with them in ternary aqueous mixtures. Amines become electrically charged in water [60], thereby facilitating their interactions with taurine. With most amines analyzed, the amines contribute bands which are overlapped with the SO stretch bands of taurine, rendering the analysis of the SO band challenging (Fig. 1 and Fig. S4, supporting information file). This is however not the case with AEE, which has an effect opposite to that of water on the SO band of taurine (i.e., with AEE and water, the SO stretch band of taurine shifts to lower numbers, Fig. 1). This result suggests that, in aqueous solutions, the SO groups of taurine interact with AEE more strongly than they would interact with other taurine molecules in dry taurine. Despite the band overlap, a similar effect is qualitatively seen with DIPA (Fig. 1). With the other amines, the band overlap does not enable observing possible shifts of the SO band of taurine (Fig. S4, supporting information file).

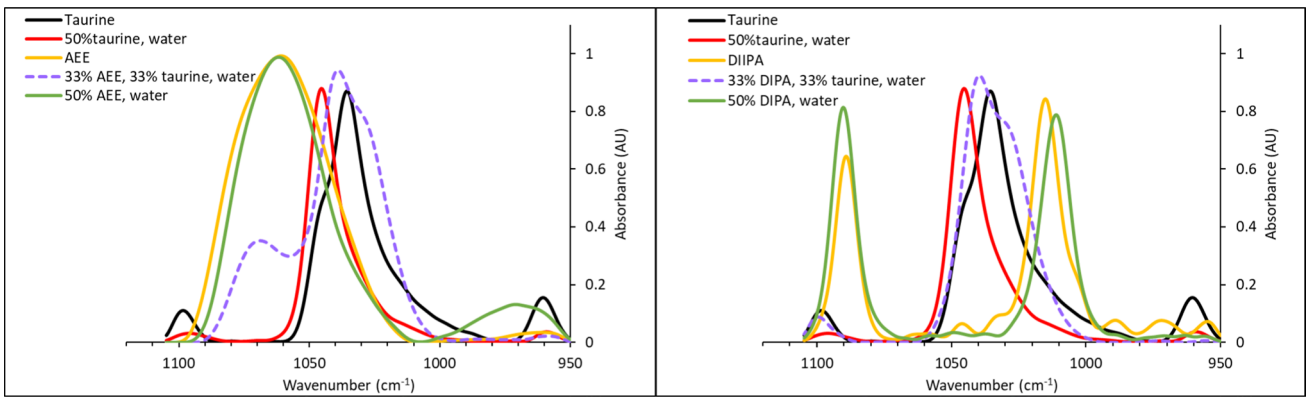

Fig. 1 ATR-FTIR spectra of amines and their mixtures in the 950–1100^{-1} region, for binary mixtures with water (50wt% amine in water), and in ternary mixtures with taurine (at a 1:1:1 wt. ratio of taurine:amine:water). The spectra of taurine and 50% taurine in water are also shown in each panel. The SO band of taurine is seen in this region, and used to interpret taurine interactions with water and amines in aqueous solutions. The SO band of neat taurine is split into a peak at 1034 cm^{-1} and a shoulder at 1042 cm^{-1}, both of which are ascribed to the stretching vibration of the sulfate groups, υ (SO). The spectra for amines not shown in this figure are in the supporting information file (Fig. S3)

The SO bond also displays signatures between 1100–1300 cm^{-1}, with peaks at 1210 and 1175 cm^{-1}, as seen in Fig. 2. Previous studies ascribed the peaks at 1210 cm^{-1} and 1175 cm^{-1} to the stretching S=O vibration, υ (SO) [49, 61, 62]. The peak at 1175 cm^{-1} shifts to higher wavenumbers upon mixing with water, without amines. This result supports the hypothesis that SO-water interactions are weaker than SO-taurine interactions in the dry state, as discussed above. In aqueous mixtures of taurine with PYR, the peak at 1175 cm^{-1} shifts to even higher wavenumbers compared to binary mixtures of taurine in water, without PYR. In contrast, the peak at 1175 cm^{-1} shifts to lower wavenumbers in aqueous mixtures of taurine with all other amines. This result is indicative of interactions between amines and the oxygen of the sulfate groups of taurine, in all cases except PYR. Note that PYR has a nitrogen on its ring, but no NH groups. We cannot discount that sulfolane-PYR interactions occur through the sulfur of the SO groups of taurine and the nitrogen of PYR. A study showed the formation of PYR-SO_2 dimers, with bonds between the N of PYR and the S atom, as well as CH…OS bonds between the hydrogens of PYR and the oxygen of SO_2 [63]. Such interactions would induce a blue shift of the υ (SO) band to higher wavenumbers.

In addition to the SO band of taurine, the OH stretch band of water can, in principle, be used to obtain indirect evidence of amine-taurine interactions, in binary taurine-water mixtures. We investigate this band with DIPA and the other alkanolamines. In the absence of amines, despite the fact that water interacts with taurine, the effect on the υ (OH) stretch bands is negligible (Fig. 3). Similar observations apply to the υ (OD) band of D_2O, upon mixing with taurine (Fig. 3). This result may seem surprising, since the OH stretch band of water is very sensitive to H bonding [64]. Recall, however, that interactions between taurine and water occur through both the SO and the NH groups of taurine, which act as H bond acceptors and donors, respectively. As a result, the proportion of different water species (i.e., water molecules coordinated in different ways to other molecules in solution [64]) would remain unaltered.

We use D_2O instead of water to gain insights regarding molecular interactions in ternary aqueous mixtures of taurine and amines. The NH and OH stretch bands of the amines and are overlapped with OH stretch band of water at 2500–3700 cm^{-1}. In contrast, the DO stretch band of D_2O has no overlap with the NH stretch band of DIPA or the OH stretch band of the other amines. Therefore, we analyze the effect of amines and taurine on this band, comparing it to the effect of taurine alone and the amines alone (Fig. 3, and Figs. S1-S2 and Tables S1-S5, supporting information file). While taurine does not distort the DO stretch band of D_2O, DIPA distorts this band, increasing the relative area underneath the peaks at the lowest wavenumbers, while decreasing the relative area of peaks at the high and mid wavenumbers (Fig. 3). With taurine and DIPA, this effect is more marked compared to DIPA only. Previous research conducted using D_2O reports that peaks at the lowest wavenumbers correspond to more structured (ice-like) D_2O, those at intermediate wavenumbers to liquid D_2O and finally those at the highest wavenumbers to weakly hydrogen bonded D_2O [65]. These results suggest that in ternary mixtures of D_2O, DIPA and taurine, DIPA forms clusters with taurine (via NH…OS hydrogen bonds). We propose that DIPA-taurine clusters interact differently with water compared to either taurine alone or DIPA alone. DIPA-taurine clusters are likely more hydrophobic than DIPA alone, because the NH groups of DIPA would not be available for interactions with water, leaving only the CH groups exposed. A previous study reports that hydrophobic surfaces are more effective in orienting (i.e., structuring) water molecules close to aqueous-hydrophobic interfaces [66], consistent with our hypothesis and results. We will further discuss the hydrophobicity of taurine-DIPA clusters later, in light of the effect of taurine on the solubility of DIPA in water (cf. Figures 5, 6).

Dissimilar to observations with DIPA, with other amines we not observe marked differences between the DO stretch band of D_2O in binary amine-water mixtures compared to ternary mixtures containing amines, taurine and D_2O (Fig. S4, supporting information file). We propose that this result is due to the greater hydrophobicity of DIPA-taurine clusters, compared to clusters formed by taurine with the other amines, which are alkanolamines. DIPA can interact with water or D_2O through the NH group, but this interaction would be hampered by preferential interactions between the sulfate group of taurine and the NH group of DIPA. While DIPA does not have OH groups, the OH groups of the alkanolamines can also interact with water. This can decrease the effect of taurine-amine interactions on the interactions between alkanolamines and water.

Finally, in Fig. 4, we can observe the δ (HNH) scissor of AMP and AEE close to the δ (HOH) band of water. In both cases, the δ (HNH) vibration shifts to higher wavenumbers in the presence of taurine (compared to aqueous solutions without taurine). This confirms that interactions occur due to H bonding of the NH groups of the amines and the sulfate groups of taurine (NH…OS). Note that the δ (HNH) band is not observed with the other amines, which have NH (as opposed to NH_2) groups or no NH groups (in the case of PYR).

In summary, the NH groups of amines can interact with the sulfate group of taurine. To our knowledge, previous studies have not analyzed amine interactions with taurine. However, NH…OS interactions have been reported for other molecules. For example, previous research ascribed to NH…OS interactions the encapsulation of sulfate anions by

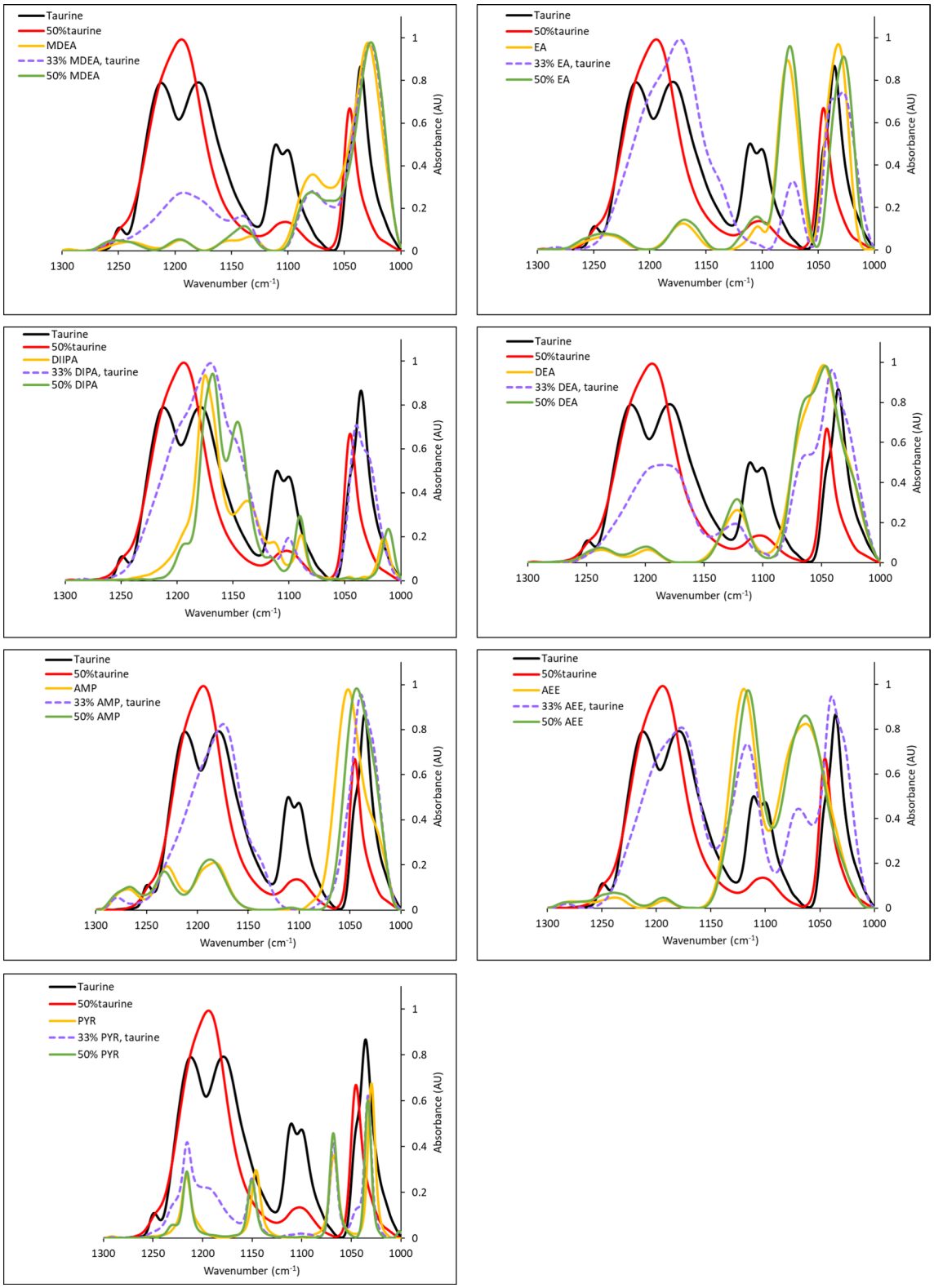

Fig. 2 ATR-FTIR spectra of amines and their mixtures in the 1100–1300 cm^{-1} region, for binary mixtures with water (50wt% amine in water), and in ternary mixtures with taurine (at a 1:1:1 wt. ratio of taurine:amine:water). The spectra of taurine and 50% taurine in water are also shown in each panel. The amines analyzed are MDEA, DIPA, EA and AMP, as well as PYR. The SO bond displays signatures between 1100 and 1300 cm^{-1}, with peaks at 1210 and 1175 cm^{-1}, which are therefore used to analyze interactions of taurine with water and amines in aqueous solution

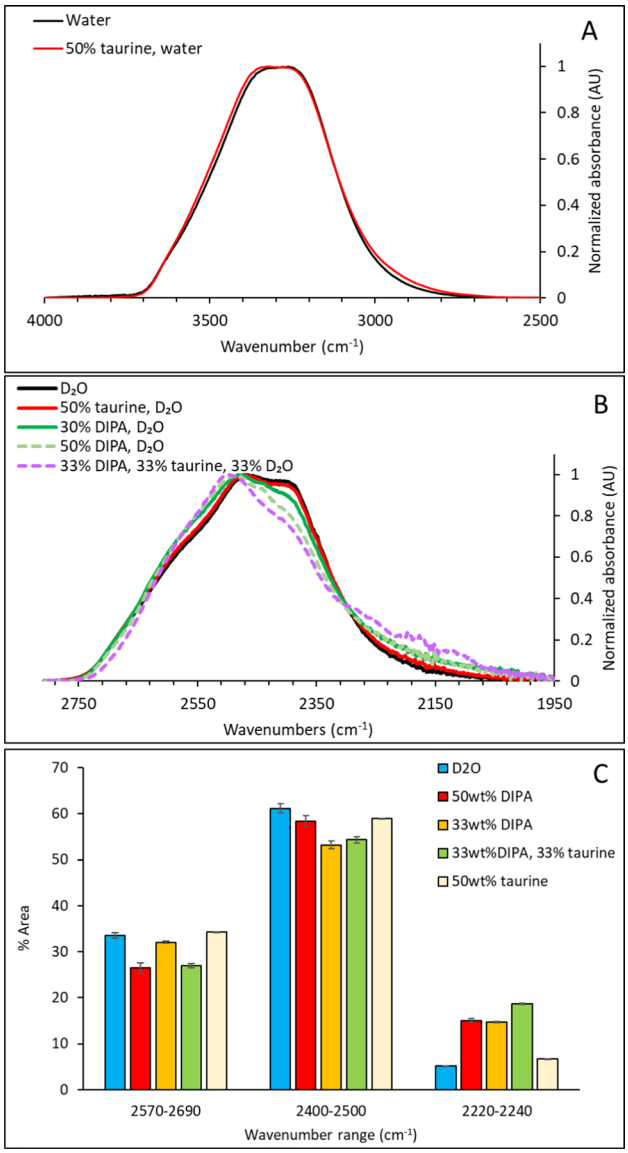

Fig. 3 ATR-FTIR absorbance spectra in the 2500–4000 cm^{-1} region, showing the υ (OH) stretch band of pure water and of water with taurine (**A**). ATR-FTIR absorbance spectra in the 1950–2800 cm^{-1} region, showing the υ (OD) stretch band of D_2O upon mixing with taurine, amines and taurine and amines (**B**). Relative area underneath the peaks at different wavenumbers, convolved under the υ (OD) stretch shown in panel **B**, using the procedure given in Sect. 2.2 (**C**). A sample deconvolution is given in the supporting information file (Fig. S1), alongside the comparison between the replicate samples (Fig. S2) and the tables showing the percent areas estimated for each of them (Tables S1-S5). The amine and taurine concentrations in each sample are expressed as weight-based percentages

thiophene-based macrocycle containing four secondary and two tertiary amines [67]. Also, a theoretical study proposed that guanidine-bisulfate complexes form due to S–O···H–N interactions (as well as O–H···N interactions) [68]. NH…OS interactions are also proposed in a study analyzing the sulfate anion recognition by peptides [69].

Recall the importance of the sulfate group of taurine on its biological function, as highlighted in the introduction. As mentioned earlier, sulfonation is important because it prevents the passive transport of taurine across membranes, due to its negative charge [2]. Taurine action on the adrenal gland is linked to its sulfonate group, rather than on its amino group [2]. Moreover, previous research indicates that taurine interacts mostly with cations rather than with anions, due to its sulfonate group [2]. It specifically interacts with divalent calcium, partaking in membrane stabilization [2]. For example, Ca^{2+} binding by taurine affects retinal membranes [70]. Interactions between amines and the sulfate group of taurine would adversely affect its transport across membranes, its ability to bind calcium ions and stabilize biological membranes, and its beneficial action on organs such as adrenal glands. Amine-taurine interaction can therefore contribute to adverse effects on the body of amines used in carbon capture and storage and to sweeten sour gas, as well as in cosmetics. IR data indicate that DIPA-taurine interactions yield clusters (aggregates) which are less soluble in water compared to free DIPA. This may also impact the toxicity of DIPA in the body, by enhancing its partitioning and bioaccumulation into fatty tissues, as further discussed in the next section.

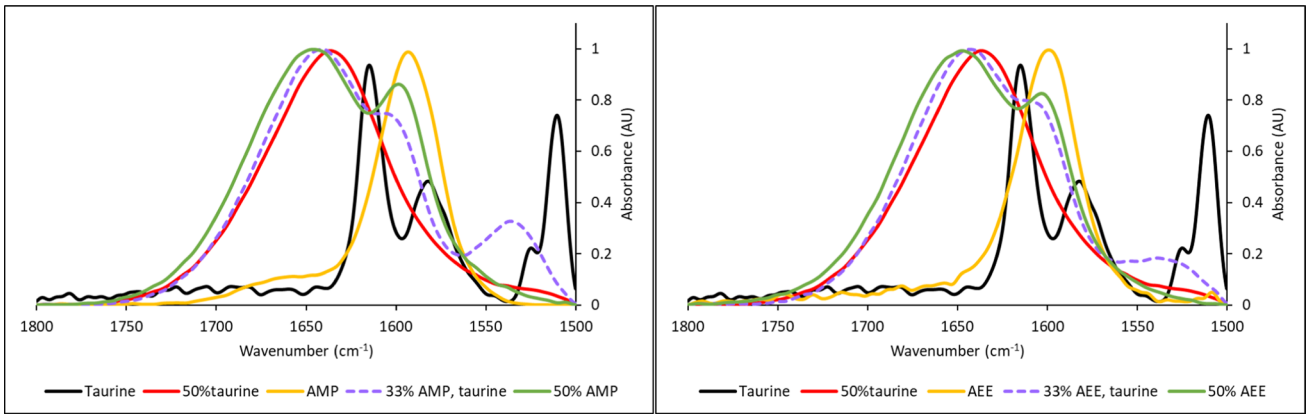

Fig. 4 ATR-FTIR spectra of amines and their mixtures in the 1500–1800 cm^{-1} region, for binary mixtures with water (50wt% amine in water), and in ternary mixtures with taurine (at a 1:1:1 wt. ratio of taurine:amine:water). The spectra of dry taurine and 50% taurine in water are also shown in each panel. We can observe the δ (HNH) scissor of AMP and AEE at ≈1600 cm^{-1}, close to the δ (HOH) band of water at ≈1650 cm^{-1}

3.2 Amine interactions with taurine: impact on mixing behaviour in binary and ternary mixtures

Bottle tests were conducted using EA, DEA, AMP, AEE, MDEA, PYR, and DIPA, to assess the effect of taurine on the mixing behaviour of amines in water.

Without taurine, all amines analyzed are freely miscible in water, with the exception of DIPA, and they yield clear aqueous solutions. In contrast, DIPA forms dispersions in water above its solubility limit; these dispersions are also optically clear [60]. Taurine (1wt%, relative to water) and amines (10 or 18 wt%) yield aqueous solutions that are clear to the naked eye in all cases (data not shown), except with DIPA. With DIPA, mixtures are initially turbid, although they become clear within 10 min (Fig. 5). This result confirms that taurine hampers mixing between DIPA and water, thereby forming larger droplets which result in the observed turbidity at short time intervals. This result is consistent with the hydrophobicity of DIPA-taurine clusters we previously discussed, based on IR data. Figure 5 shows the proposed mechanism of hydrophobic DIPA-taurine cluster formation, based on ATR-FTIR data, and compares the turbidity of 10wt% DIPA mixtures in water, with and without taurine.

The separation between DIPA and water by taurine is also highlight by optical microscopy images, taken using samples dyed with Nile red. Nile red is a hydrophobic dye, which is soluble in DIPA but not water (Fig. 6). Therefore, it partitions in DIPA-rich regions, which appear red, while water-rich regions of the sample appear dark. In Fig. 6A, with 70wt% DIPA, droplets are water-rick (dark), while the continuous phase is DIPA-rich (red). Figure 6 also shows that with 10wt% DIPA, 1wt% toluene and water, the continuous phase is instead water (dark).

Although DIPA-taurine complexes are more hydrophobic compared to complexes of taurine with the other amines (alkanolamines), light scattering reveals that taurine emulsifies all amines in water, yielding sub-micron droplets (Fig. 7). Note that the instrument used only enables observations of sub-micron droplets. Therefore, larger droplets potentially present in mixtures of DIPA, taurine and water would not be observable in these measurements.

Furthermore, we indirectly probed the hydrophobicity of amine-taurine complexes by including toluene in the mixtures. Table 1 summarizes the solubility of toluene in different amines and in water, as estimated using COSMO-RS. The solubility of toluene in DIPA, PYR and AMP is high, while being lower with all other amines. As a result, DIPA, PYR and AMP effectively emulsify toluene in water, dissimilar to the other amines analyzed. Consistent with these data, the turbidity detected with a spectrophotometer is above detection (≥ 2.5 NTU) upon mixing 1wt% toluene in aqueous mixtures containing 10wt% DIPA, PYR or AMP. Similar results are obtained in the presence of 1wt% taurine (relative to water), with either PYR or AMP. Bottle tests also showed no visible differences in toluene emulsification with and without taurine (Fig. 5).

In contrast, taurine affected toluene emulsification by DIPA. DIPA effectively emulsified toluene in water without taurine, but with 1% toluene, 1% taurine and 10% DIPA, a free layer separated from the water phase. Nonetheless, droplets could be observed immediately after agitation (Fig. 6B). The volume of the free layer observed in bottle tests exceeded that of the toluene added. This indicates that taurine favored DIPA separation from water, causing it to partition into the toluene phase. This is also evident in longer term observations, conducted with 10wt% DIPA and

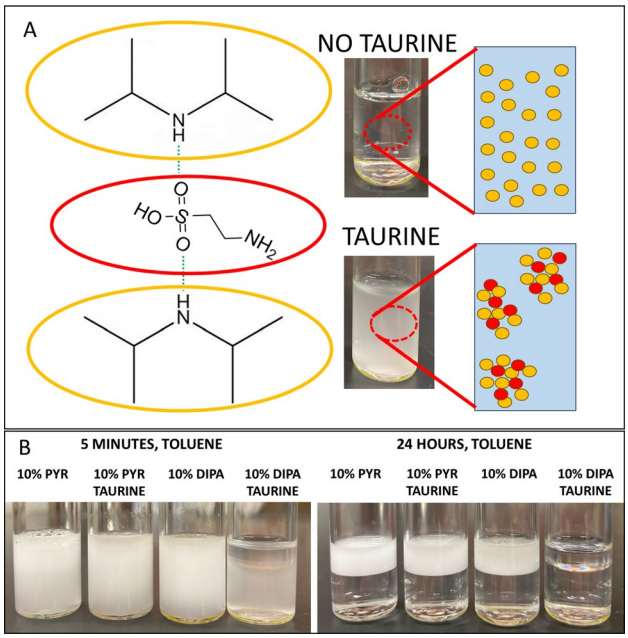

Fig. 5 **A** Bottle tests conducted with 10wt% DIPA and 1wt% taurine (relative to water), and proposed formation mechanism of hydrophobic DIPA-taurine clusters, based on ATR-FTIR data previously discussed. Pictures were taken 2 min after agitation; **B** bottle tests conducted with toluene (1:4 toluene:aq. solution, wt. based), PYR and DIPA (10wt%), and taurine (1wt%). Similar to PYR, with other amines we could not observe differences between the emulsification of toluene with and without taurine with the naked eye. Toluene emulsification was also analyzed with a spectrophotometer

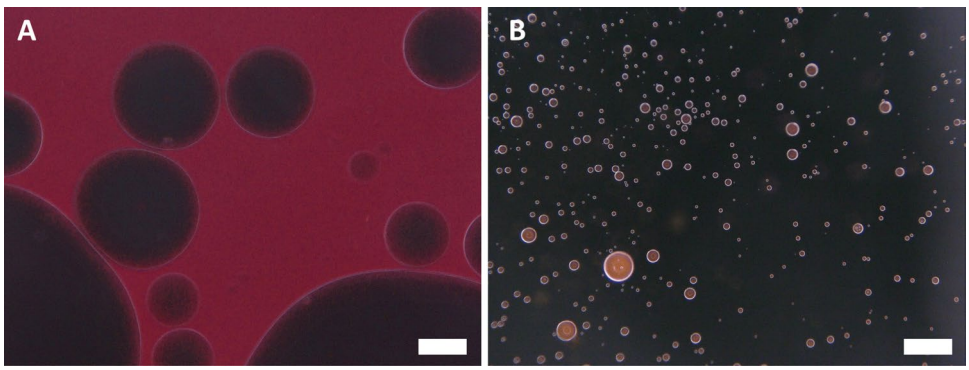

Fig. 6 Optical microscopy images of samples containing 70wt% DIPA and 2wt% taurine, relative to the water phase (**A**) and of samples containing 10wt% DIPA, 1wt% toluene and 2wt% taurine (relative to water. The scale bar is 100 μ m. Samples were stained with Nile red, to highlight hydrophobic regions (red), rich in DIPA and toluene, differentiating them from water-rich regions (black). Panel **A**: Bottle tests conducted with 10wt% DIPA and 1wt% taurine (relative to water), and proposed formation mechanism of hydrophobic DIPA-taurine clusters, based on ATR-FTIR data previously discussed. Pictures were taken 2 min after agitation; Panel **B**: bottle tests conducted with toluene (1:4 toluene:aq. solution, wt. based), PYR and DIPA (10wt%), and taurine (1wt%). Similar to PYR, with other amines we could not observe differences between the emulsification of toluene with and without taurine with the naked eye. Toluene emulsification was also analyzed with a spectrophotometer

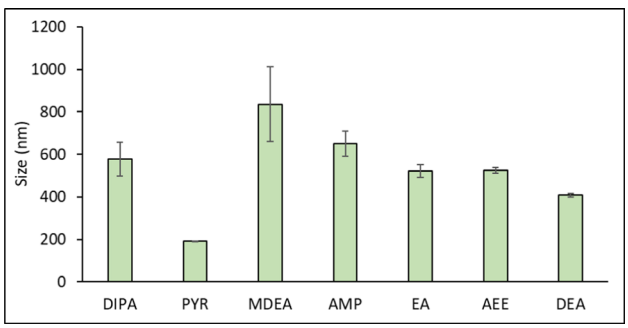

Fig. 7 Size of amine droplets in water, in samples containing 20wt% amines and 1wt% taurine, relative to the water phase, as determined by light scattering. The error bars reported are based on standard errors estimated from at least three measurements

Table 1 Solubility of toluene in different amines and in water, as estimated using COSMO-RS at 298.13 K

	Solubility (mole fraction)	Solubility (mass fraction)
DIPA	High	High
DEA	0.18340026	0.16441731
MEA	0.24459753	0.32807462
PYR	High	High
AMP	High	High
AEE	0.54190097	0.50893766
MDEA	0.37245634	0.31450462
Water	0.00012381	0.00063253

toluene (1:4 toluene:aq. solution, wt. based), as seen in Fig. 5. ATR-FTIR analysis of the top phase confirms that both toluene and DIPA are present in this layer (Fig. 8). These results support the proposed hypothesis that DIPA-taurine clusters are more hydrophobic compared to clusters of taurine and the other amines. The decreased miscibility of DIPA in the presence of taurine may affect its toxicity in the body, potentially enhancing its partitioning and bioaccumulation into fatty tissues. This risk would have to be further assessed in future research.

4 Conclusions and recommendations

The SO groups of taurine play a key role in its biological function. DIPA, AMP, AEE, DEA, EA and MDEA are used for carbon capture and to sweeten sour gas, and are found as groundwater pollutants. Amines are also used in cosmetic products.

DIPA, AMP, AEE, DEA, EA and MDEA interact with the SO groups of taurine through their NH group, with potential adverse effects on taurine function in the body. This is indicated by ATR-FTIR, which reveals a shift of the SO stretching band of taurine to lower wavenumbers upon mixing with amines and water. This is due to SO…HN hydrogen bonding. We also observe a shift of the NH_2 scissoring vibration of AMP and AEE, confirming such interactions. PYR and taurine could interact via S…N bonding.

DIPA is more hydrophobic than the other amines tested, and taurine further decreases its miscibility in water. This is seen in bottle tests, where taurine hampers DIPA dispersion in water. Optical microscopy images of samples dyed with Nile red qualitatively confirm separation the separation between DIPA (which appears red) and water (which appears dark). Also, while DIPA emulsifies toluene in water without taurine, taurine induces bulk separation between water and

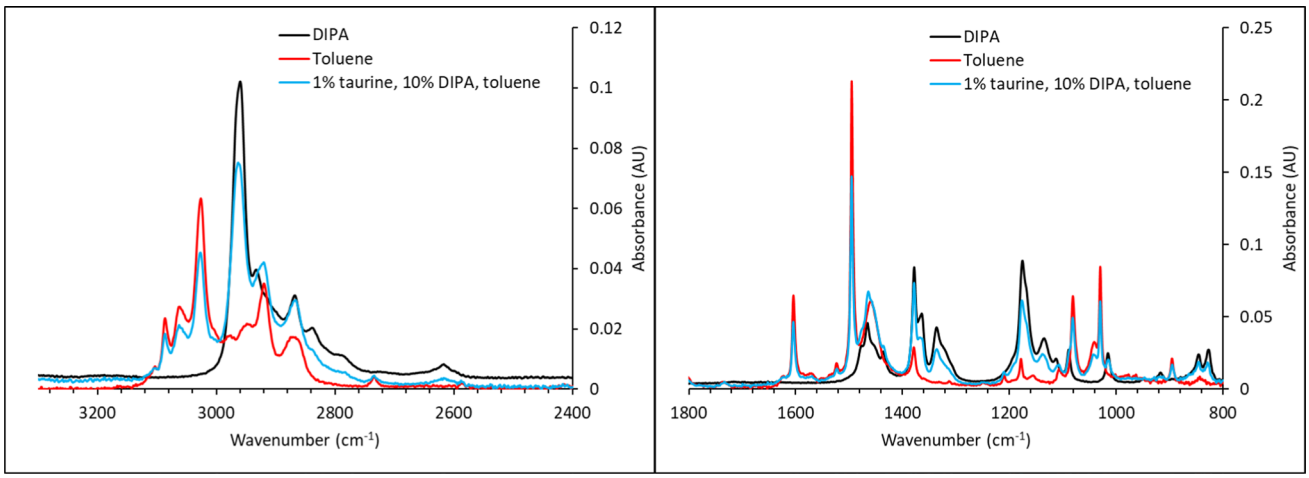

Fig. 8 ATR-FTIR analysis of the top phase of a samples containing water, with 1 wt% taurine relative to water, with 10wt% DIPA and toluene (1:4 toluene:aq. solution, wt. based). Relevant regions showing that DIPA and toluene are co-present, as indicated by the fact that both DIPA and toluene peaks appear in the spectrum of the top phase. The spectra of pure toluene and DIPA are shown as a reference

a phase containing DIPA and toluene. ATR-FTIR data indicate that hydrophobic DIPA-taurine clusters are more effective at structuring water compared to free DIPA. AMP, EA, DEA, AEE and MDEA also interact with taurine, but form less hydrophobic complexes with it compared to DIPA, likely because their OH groups can also interact with water. DIPA does not have such groups. Nonetheless, light scattering reveals sub-micron sized droplets with all amines in the presence of taurine, indicating their decreased solubility in water. Additional research is required to assess the implications of this effect on the toxicity of amines in the body. Such studies are much needed to improve on existing regulations, which allow the presence of alkanolamines and DIPA in household and cosmetic products, such as hair dyes, at concentrations well above trace percentages. These products come in direct contact with the skin for quite extended time periods (for example, typically 25–30 min in the case of hair dyes), with potential health risks to the consumers. Our future research will focus on interactions between amines and proteins, correlating it to the potential toxicity of amines on the body.

4.1 Study limitations

This study probed interactions between taurine, alkanolamines and diisopropylamine in model systems, which do not encompass the complexity of living organisms. Additional research is required to understand the toxicity of amines at the molecular and cellular level in such complex systems. Moreover, amines are often found as co-contaminants with other groundwater pollutants, which may affect amine toxicity. Future research should focus on analyzing more realistic mixtures, and observing impacts in vitro, in more complex biological systems. Animal studies will not be part of our future research.

Author contributions Erica Pensini: supervision, conceptualization, analysis and interpretation of data, investigation, writing—original draft. Nour Kashlan and Caitlyn Hsiung: investigation, writing—review and editing. All authors revised and approved the final draft.

Funding This research was funded by the Natural Sciences and Engineering Research Council of Canada (NSERC) through an NSERC Discovery grant and an NSERC Alliance grant supported Shell Canada and Shell Oil US, Matrix Solutions and Azimuth Consulting.

Data availability Data supporting this study will be made available upon request from the corresponding author.

Code availability This manuscript did not generate new code. The solubility of toluene in the different amines used was estimated using COSMO-RS, version 2023.1 [71]. COSMO-RS (http://www.scm.com) was developed by Vrije Universiteit, Amsterdam. ATR-FTIR spectra were processed using Quasar Orange, which is a freely available software [46, 47]. Excel was used to fit normalized IR spectra to a sum of Gaussian peaks, using the Excel solver function. Any additional information required to reanalyze the data reported in this work paper is available from the corresponding author upon request.

Declarations

Competing interests The authors have no competing interests and competing interests to declare.

Open Access This article is licensed under a Creative Commons Attribution-NonCommercial-NoDerivatives 4.0 International License, which permits any non-commercial use, sharing, distribution and reproduction in any medium or format, as long as you give appropriate credit to the original author(s) and the source, provide a link to the Creative Commons licence, and indicate if you modified the licensed material. You do not have permission under this licence to share adapted material derived from this article or parts of it. The images or other third party material in this article are included in the article's Creative Commons licence, unless indicated otherwise in a credit line to the material. If material is not included in the article's Creative Commons licence and your intended use is not permitted by statutory regulation or exceeds the permitted use, you will need to obtain permission directly from the copyright holder. To view a copy of this licence, visit http://creativecommons.org/licenses/by-nc-nd/4.0/.

References

1. Schaffer SW, Ito T, Azuma J. Clinical significance of taurine. Amino Acids. 2014;46:1147.
2. Taurine 6, Springer2006.
3. Chesney MDRW. Taurine: its biological role and clinical implications. Adv Pediatr. 1985;32:1–42.
4. Lambert IH, Kristensen DM, Holm JB, Mortensen OH. Physiological role of taurine—from organism to organelle. Acta Physiol. 2015;213:191–212.
5. Seidel U, Huebbe P, Rimbach G. Taurine: a regulator of cellular redox homeostasis and skeletal muscle function. Mol Nutr Food Res. 2019;63:1800569.

6. Militante JD, Lombardini JB. Taurine: evidence of physiological function in the retina. Nutr Neurosci. 2002;5:75–90.
7. Hansen SH, Andersen ML, Cornett C, Gradinaru R, Grunnet N. A role for taurine in mitochondrial function. J Biomed Sci. 2010;17:S23.
8. Wu J, Prentice H. Role of taurine in the central nervous system. J Biomed Sci. 2010;17:S1.
9. Chen C, Xia S, He J, Lu G, Xie Z, Han H. Roles of taurine in cognitive function of physiology, pathologies and toxication. Life Sci. 2019;231: 116584.
10. Wang L, Zhao N, Zhang F, Yue W, Liang M. Effect of taurine on leucocyte function. Eur J Pharmacol. 2009;616:275–80.
11. Jonathan L, Kolawole T, Attidekou P. Carbon capture from a simulated flue gas using a rotating packed bed adsorber and mono ethanol amine (MEA). Energy Procedia. 2017;114:1834–40.
12. Wanderley RR, Ponce GJ, Knuutila HK. Solubility and heat of absorption of CO2 into diisopropylamine and N, N-diethylethanolamine mixed with organic solvents. Energy Fuels. 2020;34:8552–61.
13. Schulze-Hulbe A, Shaahmadi F, Burger AJ, Cripwell JT. Toward nonaqueous alkanolamine-based carbon capture systems: parameterizing amines, secondary alcohols, and carbon dioxide-containing systems in s-SAFT-γ Mie. Ind Eng Chem Res. 2023;62:14061–83.
14. Dawodu OF, Meisen A. Effects of composition on the performance of alkanolamine blends for gas sweetening. Chem Eng Commun. 1996;144:103–12.
15. Hawthorne SB, Kubátová A, Gallagher JR, Sorensen JA, Miller DJ. Persistence and biodegradation of monoethanolamine and 2-propanolamine at an abandoned industrial site. Environ Sci Technol. 2005;39:3639–45.
16. Luther SM, Dudas MJ, Fedorak PM. Sorption of sulfolane and diisopropanolamine by soils, clays and aquifer materials. J Contam Hydrol. 1998;32:159–76.
17. Mrklas O, Chu A, Lunn S. Determination of ethanolamine, ethylene glycol and triethylene glycol by ion chromatography for laboratory and field biodegradation studies. J Environ Monit. 2003;5:336–40.
18. Headley JV, Dickson LC, Peru KM. Comparison of levels of sulfolane and diisopropanolamine in natural wetland vegetation exposed to gas-condensate contaminated ground water. Commun Soil Sci Plant Anal. 2002;33:3531–44.
19. Shin KO, Lee YM. Simultaneous analysis of mono-, di-, and tri-ethanolamine in cosmetic products using liquid chromatography coupled tandem mass spectrometry. Arch Pharmacal Res. 2016;39:66–72.
20. Steinemann AC. Fragranced consumer products and undisclosed ingredients. Environ Impact Assess Rev. 2009;29:32–8.
21. Williams BW, Shurney GA. Hair coloring compositions. USA: Universal Beauty Products Inc; 2010.
22. Miczewski MJ, Vena LAC, Narasimhan S. Hair color compositions and methods for coloring hair. USA: Revlon Consumer Products LLC; 2006.
23. N.R. Forbes, E. Galley, C. Sheard, improved oxidative hair dyes, Europe, 2012.
24. M. Morelli, C. Dupressoir, S. David, Composition containing ethanolamine derivatives and citric acid, Worldwide, 2004.
25. Kako J, Ogihara M, Suma M. Emulsion composition for skin. USA: Otsuka Pharmaceutical Co Ltd; 2016.
26. Kwak YB, Choi MS. Identification of a metabolite for the detection of the hydrophilic drug Diisopropylamine for doping control. J Pharm Biomed Anal. 2023;234: 115576.
27. Smith FX. Ophthalmic and contact lens solutions using choline. USA: FXS Ventures LLC; 2017.
28. Pang SNJ. Final report on the safety assessment of diisopropylamine. J Am Coll Toxicol. 1995;14:182–92.
29. Doro F. On improving the climate change impact of surfactant-based cleaning products: Were you aware of the potential impact of fragrances? Colloids Surf C. 2024;2: 100027.
30. Myers RC, Ballantyne B. Comparative acute toxicity and primary irritancy of various classes of amines. Toxic Sub Mech. 1997;16:151–94.
31. Gagnaire F, Azim S, Bonnet P, Simon P, Guenier JP, De Ceaurriz J. Nasal irritation and pulmonary toxicity of aliphatic amines in mice. J Appl Toxicol. 1989;9:301–4.
32. Grant RL, Taiwo SO, McCant D. Assessment of chronic inhalation non-cancer toxicity for diethylamine. Inhalation Toxicol. 2015;27:778–86.
33. Hansen BH, Altin D, Booth A, Vang SH, Frenzel M, Sørheim KR, Brakstad OG, Størseth TR. Molecular effects of diethanolamine exposure on Calanus finmarchicus (Crustacea: Copepoda). Aquat Toxicol. 2010;99:212–22.
34. Leung HW, Ballantyne B. Developmental toxicity study with N-methyldiethanolamine by repeated cutaneous application to CD rats. J Toxicol Cutan Ocul Toxicol. 1998;17:179–90.
35. Leung HW, Ballantyne B, Frantz SW. Pharmacokinetics of Nmethyldiethanolamine following acute cutaneous and intravenous dosing in the rat. J Toxicol-Cutan Ocul Toxicol. 1996;15:343–53.
36. Ballantyne B, Leung HW. Acute toxicity and primary irritancy of alkylalkanolamines. Vet Hum Toxicol. 1996;38:422–6.
37. Leung HW, Blaszcak BS. Skin sensitization potential of four alkylalkanolamines. Vet Hum Toxicol. 1998;40:65–7.
38. Knaak JB, Leung HW, Stott WT, Busch J, Bilsky J. Toxicology of mono-, di-, and triethanolamine. Rev Environ Contam Toxicol. 1997;149:1.
39. Weeks MH, Downing TO, Musselman NP, Carson TR, Groff WA. The effects of continuous exposure of animals to ethanolamine vapor. Am Ind Hyg Assoc J. 1960;21:374–81.
40. J.B. Knaak, H.W. Leung, W.T. Stott, J. Busch, J. Bilsky, Toxicology of mono-, di-, and triethanolamine, Reviews of Environmental Contamination and Toxicology: Continuation of Residue Reviews, (1997) 1–86.
41. Mankes RF. Studies on the embryopathic effects of ethanolamine in Long-Evans rats: preferential embryopathy in pups contiguous with male siblings in utero. Teratogen Carcinogen Mutagen. 1986;6:403–17.
42. McDonald JD, Kracko D, Doyle-Eisele M, Garner CE, Wegerski C, Senft A, Knipping E, Shaw S, Rohr A. Carbon capture and sequestration: an exploratory inhalation toxicity assessment of amine-trapping solvents and their degradation products. Environ Sci Technol. 2014;48:10821–8.
43. M. Låg, Å. Andreassen, C. Instanes, B. Lindeman, Health effects of different amines relevant for CO_2 capture Nasjonalt folkehelseinstitutt, Nydalen, 2009.
44. Saghir SA, Clark AJ, McClymont EL, Staley JL. Pharmacokinetics of aminomethylpropanol in rats following oral and a novel dermal study design. Food Chem Toxicol. 2008;46:678–87.
45. Spare the animals and explore the alternatives, Nature, 631 (2024) 481.
46. Demšar J, Curk T, Erjavec A, Gorup Č, Hočevar T, Milutinovič M, Možina M, Polajnar M, Toplak M, Starič A, Štajdohar M. Data mining toolbox in python. J Mach Learn Res. 2013;14:2349–53.

47. Toplak M, Read ST, Sandt C, Borondics F. Quasar: easy machine learning for biospectroscopy. Cells. 2021;10:2300.
48. Pan Y, Tikekar RV, Wang MS, Avena-Bustillos RJ, Nitin N. Effect of barrier properties of zein colloidal particles and oil-in-water emulsions on oxidative stability of encapsulated bioactive compounds. Food Hydrocolloids. 2015;43:82–90.
49. Bruździak P, Panuszko A, Kaczkowska E, Piotrowski B, Daghir A, Demkowicz S, Stangret J. Taurine as a water structure breaker and protein stabilizer. Amino Acids. 2018;50:125–40.
50. Noguchi T, Nojiri M, Takei KI, Odaka M, Kamiya N. Protonation structures of Cys-sulfinic and cys-sulfenic acids in the photosensitive nitrile hydratase revealed by fourier transform infrared spectroscopy. Biochemistry. 2003;42:11642–50.
51. Frost RL, Kristof J, Horvath E, Kloprogge JT. Molecular structure of dimethyl sulfoxide in DMSO-intercalated kaolinites at 298 and 77 K. J Phys Chem A. 1999;103:9654–60.
52. Dai Y, Wang Y, Huang Z, Wang H, Yu L. Microsolvation effect and hydrogen-bonding pattern of taurine-water TA-(H2O)n (n = 1–3) complexes. J Mol Model. 2012;18:265–74.
53. Song IK, Kang YK. Conformational preferences of taurine in the gas phase and in water. Comput Theor Chem. 2013;1025:8–15.
54. Smit WJ, Van Dam EP, Cota R, Bakker HJ. Caffeine and taurine slow down water molecules. J Phys Commun. 2019;3: 025010.
55. Pradier CM, Dubot P. Adsorption and reactivity of sulfur dioxide on Cu(110). Influence of oxidation and hydroxylation of the surface. J Phys Chem B. 1998;102:5135–44.
56. Bartokova B, Marangoni AG, Laredo T, Pensini E. Phase behavior of sulfolane: potential implications for transport in groundwater. Colloids Surf A. 2023;677: 132451.
57. Pensini E, Marangoni AG, Bartokova B, Fameau AL, Corradini MG, Stobbs JA, Arthur Z, Prévost S. Sulfolane clustering in aqueous saline solutions. Phys Fluids. 2024;36: 037117.
58. Wang Y, Wang T, Bu S, Zhu J, Wang Y, Zhang R, Hong H, Zhang W, Fan J, Zhi C. Sulfolane-containing aqueous electrolyte solutions for producing efficient ampere-hour-level zinc metal battery pouch cells. Nat Commun. 2023;14:1828.
59. Wang Y, Wang T, Dong D, Xie J, Guan Y, Huang Y, Fan J, Lu YC. Enabling high-energy-density aqueous batteries with hydrogen bond-anchored electrolytes. Matter. 2022;5:162–79.
60. Sing M, Marangoni AG, Pensini E. Mixing behavior and electrical conductivity of diisopropyl amine-water surfactantless emulsions: implications for the electrokinetic purification of water. Colloids and Surfaces C. 2023;2:100026.
61. Benbow NL, Rozenberga L, McQuillan AJ, Krasowska M, Beattie DA. ATR FTIR Study of the Interaction of TiO2 Nanoparticle Films with β-Lactoglobulin and Bile Salts. Langmuir. 2021;37:13278–90.
62. Ghazaryan VV, Fleck M, Petrosyan AM. Mixed salts of amino acids with different anions. J Cryst Growth. 2013;362:182–8.
63. Keller JW. Sulfur dioxide-pyridine dimer. FTIR and theoretical evidence for a low-symmetry structure. J Phys Chem A. 2015;119:10390.
64. Bartokova B, Laredo T, Marangoni AG, Pensini E. Mechanism of tetrahydrofuran separation from water by stearic acid. J Mol Liq. 2023;391:123262.
65. Mudalige A, Pemberton JE. Raman spectroscopy of glycerol/D_2O solutions. Vib Spectrosc. 2007;45:27–35.
66. Hore DK, Walker DS, Richmond GL. Water at hydrophobic surfaces: when weaker is better. J Am Chem Soc. 2008;130:1800–1.
67. Saeed MA, Powell DR, Fronczek FR, Hossain MA. Cooperative NH···O and CH···O interactions for sulfate encapsulation in a thiophene-based macrocycle. Tetrahedron Lett. 2010;51:4233–6.
68. Rozas I, Kruger PE. Theoretical Study of the Interaction between the Guanidinium Cation and Chloride and Sulfate Anions. J Chem Theory Comput. 2005;1:1055–62.
69. Sheet T, Banerjee R. Sulfate ion interaction with 'anion recognition' short peptide motif at the N-terminus of an isolated helix: a conformational landscape. J Struct Biol. 2010;171:345–52.
70. Liebowitz SM, Lombardini JB, Allen CI. Sulfone analogues of taurine as modifiers of calcium uptake and protein phosphorylation in rat retina. Biochem Pharmacol. 1989;38:399–406.
71. Pye CC, Ziegler T, van Lenthe E, Louwen JN. An implementation of the conductor-like screening model of solvation within the Amsterdam density functional package. Part II. COSMO for real solvents. Can J Chem. 2009;87:790.

Publisher's Note Springer Nature remains neutral with regard to jurisdictional claims in published maps and institutional affiliations.